



# Shifts in structural diversity of Amazonian forest edges detected using terrestrial laser scanning

Eduardo Eiji Maeda, Matheus Henrique Nunes, Kim Calders, Yhasmin Mendes De Moura, Pasi Raumonen, Hanna Tuomisto, Philippe Verley, Gregoire Vincent, Gabriela Zuquim, José Luís Camargo

## ► To cite this version:

Eduardo Eiji Maeda, Matheus Henrique Nunes, Kim Calders, Yhasmin Mendes De Moura, Pasi Raumonen, et al.. Shifts in structural diversity of Amazonian forest edges detected using terrestrial laser scanning. *Remote Sensing of Environment*, 2022, 271, 11 p. 10.1016/j.rse.2022.112895 . hal-03545236

HAL Id: hal-03545236

<https://hal.inrae.fr/hal-03545236>

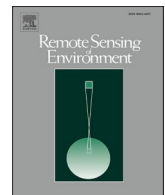
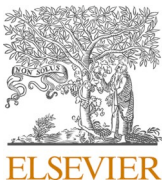
Submitted on 27 Jan 2022

**HAL** is a multi-disciplinary open access archive for the deposit and dissemination of scientific research documents, whether they are published or not. The documents may come from teaching and research institutions in France or abroad, or from public or private research centers.

L'archive ouverte pluridisciplinaire **HAL**, est destinée au dépôt et à la diffusion de documents scientifiques de niveau recherche, publiés ou non, émanant des établissements d'enseignement et de recherche français ou étrangers, des laboratoires publics ou privés.



Distributed under a Creative Commons Attribution 4.0 International License



## Shifts in structural diversity of Amazonian forest edges detected using terrestrial laser scanning



Eduardo Eiji Maeda <sup>a,j,\*</sup>, Matheus Henrique Nunes <sup>a</sup>, Kim Calders <sup>b</sup>,  
Yhasmin Mendes de Moura <sup>c,d</sup>, Pasi Raumonen <sup>e</sup>, Hanna Tuomisto <sup>f</sup>, Philippe Verley <sup>g</sup>,  
Gregoire Vincent <sup>g</sup>, Gabriela Zuquim <sup>f,h</sup>, José Luís Camargo <sup>i</sup>

<sup>a</sup> Department of Geosciences and Geography, P.O. Box 68, FI-00014 University of Helsinki, Finland

<sup>b</sup> CAVElab — Computational and Applied Vegetation Ecology, Department of Environment, Faculty of Bioscience Engineering, Ghent University, Coupure Links 653, 9000 Ghent, Belgium

<sup>c</sup> Institute of Geography and Geoecology, Karlsruhe Institute of Technology (KIT), Kaiserstr. 12, 76131 Karlsruhe, Germany

<sup>d</sup> Centre for Landscape and Climate Research, School of Geography, Geology and the Environment, University of Leicester, Leicester LE17RH, United Kingdom

<sup>e</sup> Mathematics, Tampere University, Korkeakoulunkatu 7, 33720 Tampere, Finland

<sup>f</sup> Department of Biology, University of Turku, Finland

<sup>g</sup> AMAP, University of Montpellier, CIRAD, CNRS, INRAE, IRD, 34000 Montpellier, France

<sup>h</sup> Section for Ecoinformatics and Biodiversity, Department of Biology, Aarhus University, Denmark

<sup>i</sup> Biological Dynamics of Forest Fragment Project (BDFFP), National Institute for Amazonian Research (INPA). 2936, Av. André Araújo, 69067-375 Manaus, AM, Brazil

<sup>j</sup> School of Biological Sciences, Faculty of Science, University of Hong Kong, Hong Kong, SAR

### ARTICLE INFO

Editor: Jing M. Chen

#### Keywords:

Forest fragmentation

Tropical forests

LIDAR

Structural traits

### ABSTRACT

Forest edges are an increasingly common feature of Amazonian landscapes due to human-induced forest fragmentation. Substantial evidence shows that edge effects cause profound changes in forest biodiversity and productivity. However, the broader impacts of edge effects on ecosystem functioning remain unclear. Assessing the three-dimensional arrangement of forest elements has the potential to unveil structural traits that are scalable and closely linked to important functional characteristics of the forest. Using over 600 high-resolution terrestrial laser scanning measurements, we present a detailed assessment of forest structural metrics linked to ecosystem processes such as energy harvesting and light use efficiency. Our results show a persistent change in forest structural characteristics along the edges of forest fragments, which resulted in a significantly lower structural diversity, in comparison with the interior of the forest fragments. These structural changes could be observed up to 35 m from the forest edges and are likely to reflect even deeper impacts on other ecosystem variables such as microclimate and biodiversity. Traits related to vertical plant material allocation were more affected than traits related to canopy height. We demonstrate a divergent response from the forest understory (higher vegetation density close to the edge) and the upper canopy (lower vegetation density close to the edge), indicating that assessing forest disturbances using vertically integrated metrics, such as total plant area index, can lead to an erroneous interpretation of no change. Our results demonstrate the strong potential of terrestrial laser scanning for benchmarking broader-scale (e.g. airborne and space-borne) remote sensing assessments of forest disturbances, as well as to provide a more robust interpretation of biophysical changes detected at coarser resolutions.

### 1. Introduction

Forest fragmentation has a pervasive influence on the composition of tropical ecosystems. Under the influence of edge effects, forests experience accelerated mortality of large trees (Laurance et al., 2000), causing shifts in floristic composition within hundreds of meters from

the fragment edges (Laurance et al., 2006). Fragmented forests have more abiotically dispersed plant species and fewer animal-dispersed species than continuous forests, and altered tree size distribution (Laurance et al., 2018, 2006). These changes have substantial impacts on the carbon cycle, leading to an additional emission of 0.34Gt of carbon per year, which represents almost one third of the currently

\* Corresponding author at: School of Biological Sciences, Faculty of Science, University of Hong Kong, Hong Kong, SAR

E-mail address: [eduardo.maeda@helsinki.fi](mailto:eduardo.maeda@helsinki.fi) (E.E. Maeda).

estimated annual carbon releases due to deforestation in the tropics (Brinck et al., 2017; Silva Junior et al., 2020).

Disturbances in tropical forest edges are likely to have a substantial global impact. Currently, approximately 20% of tropical forests are located within 100 m of a forest edge (Brinck et al., 2017). As forest loss continues, the size of remaining fragments tends to decline (Hansen et al., 2020) and the length of open forest edges to increase (Brinck et al., 2017). It is estimated that less than 40% of the remaining tropical forests have high ecosystem integrity (Grantham et al., 2020). The integrity of an ecosystem can be generally defined as a measure of how much a system is free from human induced changes of its structure, composition, and function (Parrish et al., 2003).

As deforestation moves landscapes towards more fragmented configurations and increases edge area, it is crucial to clarify how ecosystems will adapt to these new scenarios and define the upcoming decisions on the sustainability of tropical forests (Barlow et al., 2018). Despite the demonstrated influence of edge effects on floristic composition and carbon storage (Laurance et al., 2002; Ordway and Asner, 2020; Silva Junior et al., 2020; Tabarelli et al., 2004), less is known about the long-term effects of forest fragmentation on ecosystem functioning, structure, ecological traits and processes. As a consequence, we still lack a comprehensive understanding of how fragmentation affects ecosystem integrity in tropical regions.

Important challenges exist in working towards a deeper understanding of the broad-scale impacts caused by forest fragmentation, including uncertainty in how to quantify them and the sheer size and complexity of tropical ecosystems. Approaches based on the remote measurement of forest structural characteristics are a promising avenue to overcome these challenges, as the individuals of a community can be described in relation to their distribution in space (Fahey et al., 2019; Schneider et al., 2017). Forest structural metrics, also referred to as structural traits (Schneider et al., 2020, 2017; Verbeeck et al., 2019), have the potential to provide a spatially continuous description of forest structural diversity without the need of site-specific taxonomic information (Schneider et al., 2017; Verbeeck et al., 2019), thus allowing large scale assessments of forest disturbances.

Structural traits are strongly linked to different aspects of forest functioning, including nutrient fluxes, resource acquisition, competitive ability and growth of individuals (Enquist et al., 2009; Silva Pedro et al., 2017). Plant area and density metrics, such as plant area index (PAI), are related to aboveground biomass and land-atmosphere interactions (Reich, 2012), whereas canopy height metrics can provide information on light interception and canopy hydraulic conductivity (Reich, 2012). Structural traits can also be used to derive measures of forest structural diversity (Schneider et al., 2017). Here, we evaluate structural diversity as a combined measure of the three-dimensional variation in plant surface area in the forest. Structural diversity was suggested to be a better predictor of key ecosystem functions, such as productivity, energy, and nutrient dynamics, than biodiversity measures (LaRue et al., 2019).

Although approaches based on structural traits hold a lot of potential for understanding forest disturbances, tools to comprehensively measure these traits in dense tropical forests have so far been limited and the impacts of edge effects on forest structural diversity are not yet fully understood. Considerable progress has been made by applying airborne laser scanning, as well as portable canopy profiling LiDAR systems (PCL), which has led to a better understanding on the impacts of forest disturbances on structural characteristics, such as canopy height and above ground biomass (Almeida et al., 2019a; Stark et al., 2015). Nonetheless, these tools cannot fully capture the three-dimensional (3D) arrangement of the canopy. Airborne LiDAR systems typically acquire data with pulse densities less than a few tens per meter square and footprint sizes one or two decimetre large, which cannot fully resolve the structural arrangement of plants in tropical forests (Bazezew et al., 2018). Furthermore, due to signal occlusion in dense canopies, the return density decreases rapidly within the forest canopy and airborne

LiDAR data is unable to describe in details how plant biomass is spatially allocated in the understory of tropical forests (Heiskanen et al., 2015), even though substantial progress has been made to assess the impacts of disturbances on understory vegetation (Andersen et al., 2014; d'Oliveira et al., 2012). PCL systems partially fulfil the need for a better assessment of vertical distribution of plants. However, PCL data is two-dimensional, while the structure of canopies is inherently three-dimensional, with basic functions such as energy harvesting and light use efficiency being defined by a combination of vertical and horizontal allocation of vegetation elements (Fahey et al., 2019).

These limitations hamper the development of benchmark assessments, which are critical for robustly upscaling analysis at regional and global scales. Although airborne and spaceborne LiDAR systems will certainly play a central role in mapping forest disturbances at larger scales in the future, baseline studies are necessary to understand and validate the ecological processes that are happening on the ground (Dubayah et al., 2020).

Terrestrial laser scanning (TLS) holds strong potential for overcoming these limitations, as it can provide explicit 3D information on forest structure from the ground level (Calders et al., 2020). Since measurements are taken from within the canopy, TLS data can provide much more detailed information on the forest understory, which is extremely valuable in dense tropical vegetation. Studies applying TLS measurements have become increasingly popular in recent years, as they provide novel insights on fundamental ecological theories, and allow a more robust exploitation of models and metrics that depend on 3D structural information (Calders et al., 2020; Disney, 2019).

Here, we apply TLS measurements to evaluate structural edge effects on Amazonian forests located in the longest running fragmentation experiment in the tropics, where forest fragments have been monitored for more than 40 years (Laurance et al., 2018, 2011). We quantified structural changes in forest edges using high-definition 3D information to answer two main questions. Firstly, which forest structural traits are persistently affected by edge effects? Secondly, do changes in the three-dimensional allocation of plants impact the structural diversity of forest edges?

## 2. Material and methods

### 2.1. Study area

The study area is located north of Manaus, in Central Amazonia, Brazil. We sampled seven transects of 50 m (4 transects) and 100 m (3 transects) length, located in forest fragments of 1 ha, 10 ha and 100 ha (Fig. 1). The fragments are part of the Biological Dynamics of Forest Fragments Project Area of Relevant Ecological Interest (ARIE-BDFP), which is a collaborative research effort between the Brazilian National Institute for Amazonian Research (INPA) and the Smithsonian Tropical Research Institute (Laurance et al., 2018, 2011). The forest fragments were intentionally isolated from nearby intact forest in the early 1980s and have been monitored for physical and ecological changes approximately once every five years, aiming to investigate the effects of forest fragmentation on the Amazon ecosystem (Laurance et al., 2018, 2011). The natural vegetation in all the transects is a non-flooded tropical rainforest, which averages 28–35 m in canopy height. At the time of data acquisition, the matrix was formed by secondary growth forest with a 100 m cleared strip surrounding the forest fragments to keep the fragments isolated.

### 2.2. Terrestrial laser scanning (TLS) data acquisition

The TLS data were acquired using a RIEGL VZ-400i instrument. For this study, we used a vertical and horizontal scan resolution of 40 mdeg, which results in a point spacing of 34 mm at 50 m distance from the scanner. The beam divergence of the instrument is 0.35 mrad. The laser pulse repetition rate used was 600 kHz, allowing a measurement range

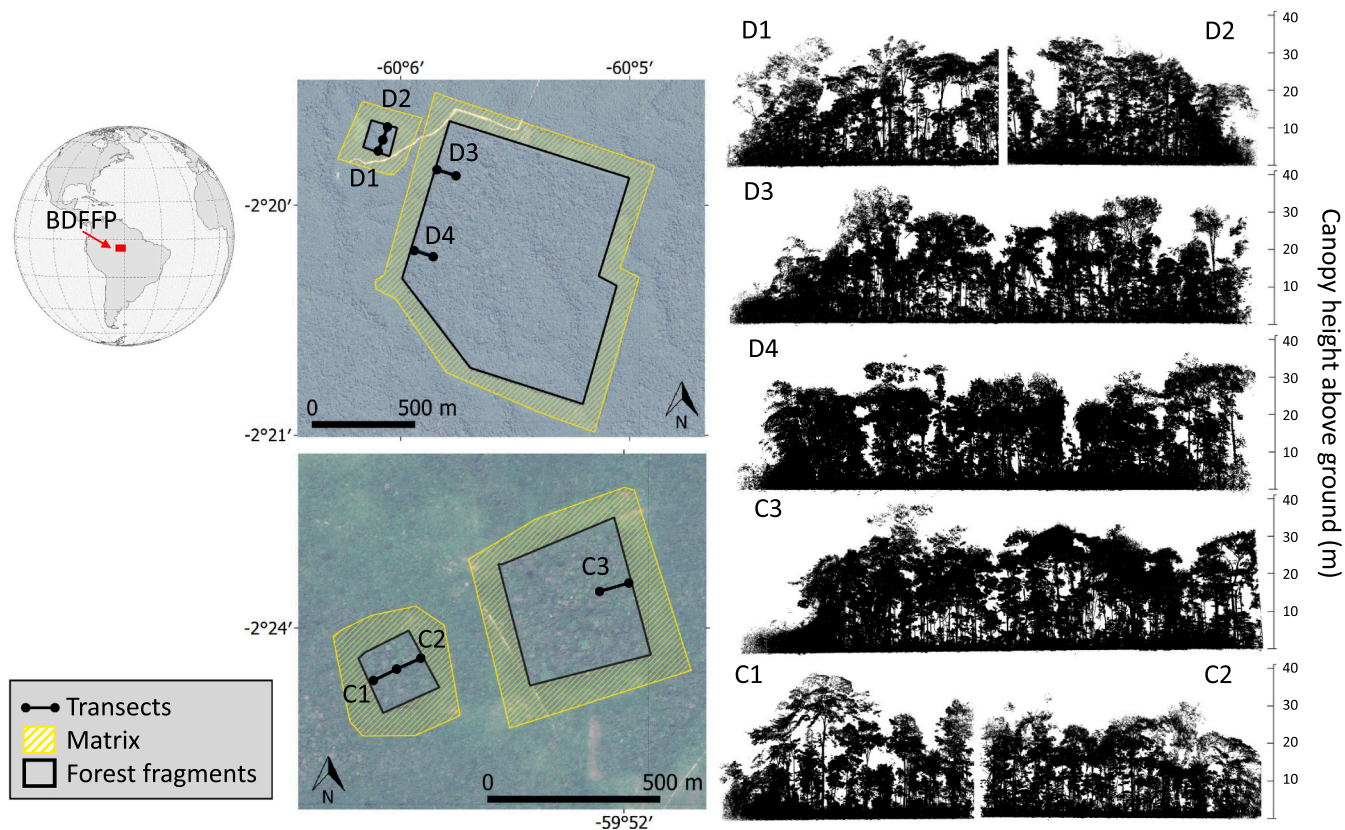


**Fig. 1.** Location of the forest fragments within the Biological Dynamics of Forest Fragments Project Area of Relevant Ecological Interest (ARIE-BDFFP) and the seven transects used in our study. The transects are marked as  $D_n$ , for transects located in the Dimona site, and as  $C_n$ , for transects located in the Colosso site, where  $n$  is the number of the transect. The figure also illustrates a vertical slice of the terrestrial laser scanning data (right column) for each of the transects.

of up to 350 m and up to eight returns per pulse.

To ensure a full 3D representation of the canopy, each transect consisted of three scan lines parallel to each other (Fig. 1 and 2a). The scans were spaced by 5 m. This spacing is much smaller than the 10–40 m usually applied in previous studies (Wilkes et al., 2017), to minimize data uncertainties due to occlusion in a dense tropical forest, as well as to maximize the acquisition of data in the upper canopy. Given that the VZ-400i scans within the zenith angle range of 30–130°, one additional measurement was acquired at each sampling position with the scanner inclined at 90° from the vertical. This resulted in a sampling of the full

hemisphere in each scan location. No co-registration targets were used in the data acquisition and the final co-registration was done in the RiSCAN PRO software version 2.9, provided by RIEGL.

### 2.3. TLS data processing

The transmittance  $T$  of a medium made-up of randomly distributed vegetation elements is commonly described as following an exponential attenuation along a path of length  $\delta$  (Nilson, 1971; Ross, 1981):

$$T = e^{-\lambda \delta} \quad (1)$$

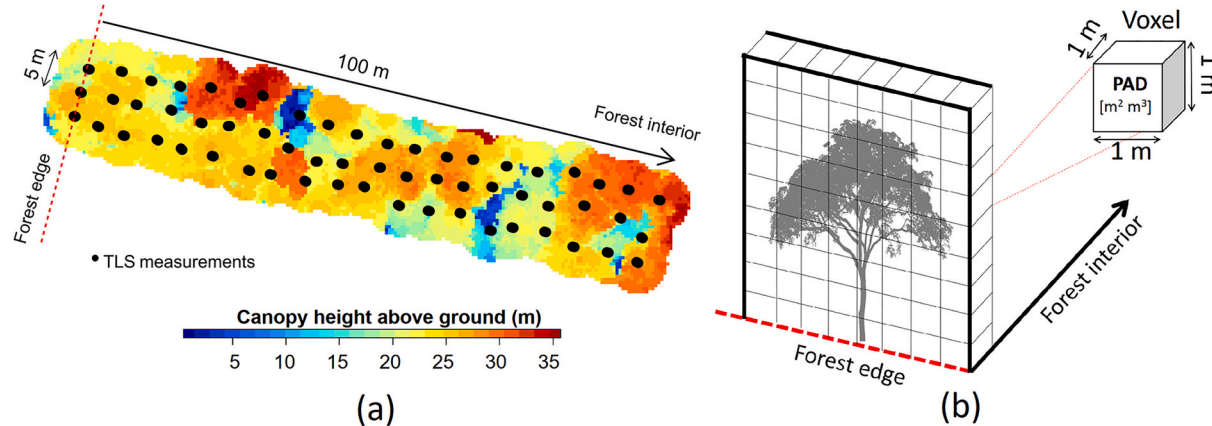


**Fig. 2.** (a) Sampling strategy for collecting the terrestrial laser scanning data along perpendicular transects to forest edges. The background image shows a canopy height model extracted from the TLS data (b) Illustration of the voxel-based approach used for assessing the three-dimensional distribution of plant area density (PAD,  $m^2 m^{-3}$ ) along the transects.

where  $\lambda$  ( $m^{-1}$ ) is the attenuation coefficient of the medium. The plant area density (PAD) ( $m^2 m^{-3}$ ) is related to  $\lambda$  as follows:

$$\text{PAD} = \lambda/G \quad (2)$$

where  $G$  is the projection coefficient function of unit plant area on a plane perpendicular to the light incident direction.

The PAD for all transects was calculated using a voxel-based approach (Fig. 2b). All transects were divided into  $1\text{ m}^3$  voxels, and the attenuation calculated for each of these voxels. This procedure was done in the LIDAR data voxelization software AMAPVox v 1.6.1 (Vincent et al., 2017). To compute PAD from attenuation,  $G$  was taken equal to 0.5, assuming a spherical distribution of vegetation elements inclination angles (Béland et al., 2011). AMAPVox tracks every laser pulse through a 3D grid (voxelized space) to the last recorded hit. The effective sampling area of each laser pulse (or fraction of pulse in case of multiple hits) is computed from the theoretical beam section (a function of distance to laser and divergence of laser beam) and the remaining beam fraction entering a voxel. In case more than one hit is recorded for a given pulse then the beam section is equally distributed between the different hits of the pulse. This information is combined with the optical path length of each pulse entering a voxel to compute the local transmittance or local attenuation per voxel. The PAD in each  $1\text{ m}^3$  voxel thus comprised every structural element of the forest, including non-tree plants such as palms, lianas and herbs.

Different estimation procedures are provided in the AMAPVox software (Vincent et al., 2021). In this study we used the free path length estimator introduced in (Pimont et al., 2018) which builds on the observation that, under the assumption of randomly distributed vegetation elements, the lengths of optical free paths, i.e. beam segments that are not intersected by vegetation elements, follow an exponential random distribution with parameter equal to the attenuation coefficient  $\lambda$ . For further details on the calculations please refer to Vincent et al. (2021) and Pimont et al. (2018). Currently, there is no clear consensus on an optimal voxels size (Grau et al., 2017; Pimont et al., 2018). In our case, a voxel space of  $1\text{ m}^3$  was considered large enough to capture the distribution of leaves and trunks, and small enough to represent the forest heterogeneity at canopy level, thus facilitating the ecological interpretation of PAD spatial arrangement. To evaluate how the voxel size affected our estimates of PAD, we carried out a sensitivity analysis with voxel sizes ranging from 0.25 m to 2 m, in an area of  $10\text{ m} \times 20\text{ m}$  of intact forest (please refer to supplementary material).

#### 2.4. Forest structural traits and their ecological significance

The PAD at each  $1\text{ m} \times 1\text{ m}$  voxel was used as base for calculating 13 forest structural traits: the Plant area index for the whole vertical column (PAI) and per 5 m height layers from 0 to 30 m height (PAI0–5, PAI5–10, PAI10–15, PAI15–20, PAI20–25, PAI25–30); Relative heights (RH) as percentiles of the vertical distribution of plant material at 25,

50, 75 and 98%; the Foliage Height Diversity (FHD); and the Canopy Ratio (CR) (Table 1). Each of these structural traits, as well as their ecological importance, are described below.

##### 2.4.1. Plant area index (PAI) for the whole vertical column and per 5 m height layers

PAI is the projected area of plant material per unit of ground area and is the combination of leaf area index (LAI) and the area of woody components including stems and branches (Vincent et al., 2017). The LAI provides an indication of the forest capacity to harvest light, exchange gases with the atmosphere and is directly related to forest-level productivity (Reich, 2012). The total PAI is, therefore, directly linked to the total light interception by plants, and high values may indicate decreased light availability under the canopy (Ma et al., 2021). Compartmentalizing PAI by vertical layers can reveal the absolute contributions of plant material to light interception and harvesting of light at the stratum level. Here, we computed the total PAI as the sum of the PAD of all voxels in a column (Almeida et al., 2019b; Vincent et al., 2017). Similarly, the PAI per 5 m height layers was calculated as the sum of the PAD of the voxels contained in each 5 m layer.

##### 2.4.2. Relative heights (RH) as percentiles of the vertical plant distribution

The heights of the plant material distribution along a vertical profile of the forest were described using relative heights (RH) (see demonstration in Fig. S1 in the supplementary material) (Dubayah et al., 2010). An RH25 of 10 m, for instance, means that 25% of plant material is below 10 m. In this study, we used the PAD in each voxel to create a vertical profile of the plant distribution in a  $1\text{ m}^2$  column, and retrieved the relative heights at the desired quantiles based on linear interpolation. Higher RH values in an  $i^{\text{th}}$  quantile can indicate 1) a lower allocation of plant material below the  $i^{\text{th}}$  threshold in comparison with forests of similar canopy height (i.e., lower regeneration of the under-story), 2) a higher allocation of plant material above the  $i^{\text{th}}$  threshold in comparison with forests of similar canopy height (i.e., branching, higher canopy packing efficiency) or 3) taller canopy height. RH is sensitive to canopy changes such as leaf loss and canopy dieback (Duong et al., 2008), and is correlated to structural attributes of the vegetation such as basal area and aboveground biomass (Drake et al., 2003). Higher canopy packing efficiency translates into a larger proportion of the canopy space being filled by plant structures and tends to be correlated with higher species richness (Jucker et al., 2015).

##### 2.4.3. Foliage height diversity (FHD)

FHD reflects the number of canopy layers and the evenness of the distribution of plant material among them in the vertical profile of the vegetation (MacArthur and MacArthur, 1961; Schneider et al., 2017; Valbuena et al., 2012). We calculated it by applying the Shannon entropy on vertical PAD profiles as proposed by MacArthur and MacArthur (1961):

$$FHD = - \sum_i p_i \times \log_e p_i \quad (3)$$

where  $p_i$  is the proportion of the total plant material that is contained within the  $i^{\text{th}}$  canopy layer.

FHD increases with increasing number of canopy layers and when the distribution of plant material becomes more even among the layers. Taking the exponential function of FHD gives the corresponding Hill number, which can be interpreted as the effective number of canopy layers (Tuomisto, 2017). We defined the layers as 5-m vertical segments of the vegetation, so their number is directly related to forest height. Higher FHD values have been linked to more diverse niches and have been used as an indicator of greater habitat complexity (Schneider et al., 2017). These metrics have also been found to correlate positively with species diversity of birds, mammals and plants (Ehlers Smith et al., 2017; Lesak et al., 2011), and to be related to bat activities (Froidevaux

**Table 1**  
Structural traits analysed in this study.

Structural trait	Acronym	Unit
Plant area index	PAI	$m^2 m^{-2}$
Plant area index from 0 to 5 m	PAI 0–5	$m^2 m^{-2}$
Plant area index from 5 to 10 m	PAI 5–10	$m^2 m^{-2}$
Plant area index from 10 to 15 m	PAI 10–15	$m^2 m^{-2}$
Plant area index from 15 to 20 m	PAI 15–20	$m^2 m^{-2}$
Plant area index from 20 to 25 m	PAI 20–25	$m^2 m^{-2}$
Plant area index from 25 to 30 m	PAI 25–30	$m^2 m^{-2}$
Relative height at 25%	RH25	m
Relative height at 50%	RH50	m
Relative height at 75%	RH75	m
Relative height at 98%	RH98	m
Canopy ratio	CR	—
Foliage Height Diversity	FHD	—

et al., 2016) and microclimate variation (Meeussen et al., 2020).

#### 2.4.4. Canopy ratio (CR)

CR is the relative difference in the heights below which 98% of the plant material (RH98) and 25% of the plant material (RH25) occur, and it is calculated as follows.

$$CR = \frac{RH98 - RH25}{RH98} \quad (4)$$

If plant material is uniformly distributed from the ground to the top of the canopy, the CR is expected to be close or equal to 0.74, as 25% of the plant material would be found between ground level and 25% of total canopy height (see demonstration in Fig. S1 in the supplementary material). CR values higher than 0.74 indicate a proportionally higher concentration of plant material in the lower layers of the canopy (the height below which 25% of plant material occurs is less than 25% of total canopy height) and CR values smaller than 0.74 indicate a proportionally higher concentration of plant material in the higher layers of the canopy. If negatively correlated with RH25, low CR indicates higher compactness of the upper strata with optimised use of canopy space combined with a less dense understory.

#### 2.5. Statistical assessment of edge effects on canopy structural traits

Each canopy structural trait was modelled as a function of distance from the edge. We compared linear mixed models containing distance from the edge with nonlinear mixed models containing an asymptotic component that represents the saturation of the canopy metric with distance from the edge. An asymptotic component in the model is more ecologically significant to investigate the edge effects on forest structure and canopy metrics (Nunes et al., 2021). We developed hierarchical models using the *lme4* package in R (Bates et al., 2015); and included the spatial levels of region of study, forest fragment size (1, 10 and 100 ha fragments) within region of study, and transect within fragment size treated as random effects to account for the nested spatial non-independence of transects. The best model, based on the Akaike Information Criterion (AIC) (Akaike, 1974), was a nonlinear mixed model  $T = \alpha^* \exp(\beta^* D) + \theta + \gamma$ ; where  $T$  is the structural trait,  $D$  is the distance from the forest edge,  $\gamma$  represents the random-effect parameters (region, fragment size, and transect location) and  $\alpha$ ,  $\beta$ ,  $\theta$  are the model coefficients. The tested models, as well as the AIC comparison are presented in the supplementary material, Table S1.

Finally, we used piecewise linear functions (hockey stick model) to identify the edge effect thresholds for those traits significantly influenced by edges based on our nonlinear mixed models. The confidence interval used for identifying the breaking points in the hockey stick model was 95%. The calculations were performed using the *SiZer* package in R (Sonderegger, 2020).

#### 2.6. Canopy structural diversity assessment using n-dimensional hypervolumes

The n-dimensional hypervolume concept for the interpretation of functional diversity provide a strong foundation for research across different fields of ecology (Blonder, 2018; Díaz et al., 2016). Here, we evaluated the structural diversity of the forest fragments through the concept of n-dimensional hypervolumes, defined by the Euclidean space formed by  $n$  independent axes (Blonder, 2018). The axes corresponded to structural traits obtained using the TLS data. To reduce the dimensionality of the hypervolumes, we used only traits that were shown to be most relevant (i.e., traits that were most influenced by edge-effects), since high-dimensional spaces can become sparse rapidly, leading to hypervolumes with data points that are disjunct. We delineated the hypervolumes using one-class support vector machine (SVM) method, which is considered insensitive to outliers and better suitable for high-dimensional hyperspaces. All calculations were done using the

*hypervolume* package in R (Blonder, 2019). For more details on the SVM approach for delineating hypervolumes, please refer to (Blonder et al., 2018).

To evaluate the changes in structural diversity caused by edge effects, we divided the combined data from all transects into slices of 5 m, from the edge to 50 m inside the forest fragments. The n-dimensional hypervolume was then calculated independently for each slice using the same dimensionality and parameters to allow a direct comparison of the hypervolumes. We then evaluated the similarity between the hypervolume of each forest slice and the hypervolume obtained at a distance of 50 m from the edge, using the Jaccard similarity index and the Sørensen similarity index, which are used to describe the pairwise overlap between hypervolumes. Given two hypervolumes A and B, the Jaccard similarity index ( $J$ ) is calculated as  $J(A,B) = |A \cap B| / |A \cup B|$ , and the Sørensen similarity index ( $S$ ) is calculated as  $S(A,B) = 2 \times |A \cap B| / (|A| + |B|)$  (Mammola, 2019). Both indices can range from 0, when the hypervolumes are fully disjunct, to 1, when the hypervolumes are identical (Mammola, 2019).

#### 2.7. Diameter at breast height (DBH) and tree density distribution

To complement the interpretation of the canopy structural traits, we analysed the tree size distribution in the transects. For that, we measured the DBH of all trees with DBH above 5 cm. The DBH measurements were extracted automatically from the TLS point cloud, following multiple steps. We first estimated the height of the points from the ground and selected the lower 5 m. Next, we defined the stems with a multi-step process that segments the point cloud into individual trees. In the segmentation we first locate cylindrical subsets that are likely real stem sections. Then we expand from the bottom of the point cloud into the trees with shortest paths. Finally, the stem sections and the shortest paths determine the individual trees. Then for each segmented tree we estimated its diameter at 1.3 m by fitting cylinders, using the least squares method. However, some segments may still contain multiple stems from different trees. To consider these cases, we tried to select subsets of points around 1.3 m with highly vertical neighborhoods. In some cases, this resulted in multiple separate components, and we fitted cylinders for all possible combinations of these components. We fitted four cylinders to each case with different weightings to get more reliable estimates. We selected the best one of the four cylinders based on the reliability of the fits. Next, we determined if cylinders are overlapping and for each group of overlapping cylinders selected the most reliable one. Finally, we filtered the selected stems using a quality assessment metric. More details of the method can be found in the supplementary material.

### 3. Results

Our analyses are based on 624 TLS measurements obtained along seven transects perpendicular to forest fragments edges (Fig. 3). The location and size of fragments, as well as idiosyncratic differences between transects, accounted for approximately 15% of the observed structural trait variability (Table S2, supplementary material). While the size of the forest fragments had a negligible effect on the results, the location of the transects accounted for approximately 10% of the structural traits variability. Hence, variations caused by distance from edge were the major driver of the spatial patterns described here.

When compared to the centre of the forests, we observed a decrease in all relative heights in the edges, at distances up to 20 m far from the forest edges. Mean RH at 98%, which provides a good representation of canopy height, decreased by approximately 4 m from the interior (at 50 m distance from edge) towards the edge of the forest fragment. The decrease in RH was also observed at 25th and 50th percentiles, indicating a relatively higher concentration of vegetation surface density in the lower strata of forests in the proximity of edges.

Edge effects caused an increase in PAI on the lower layers of the

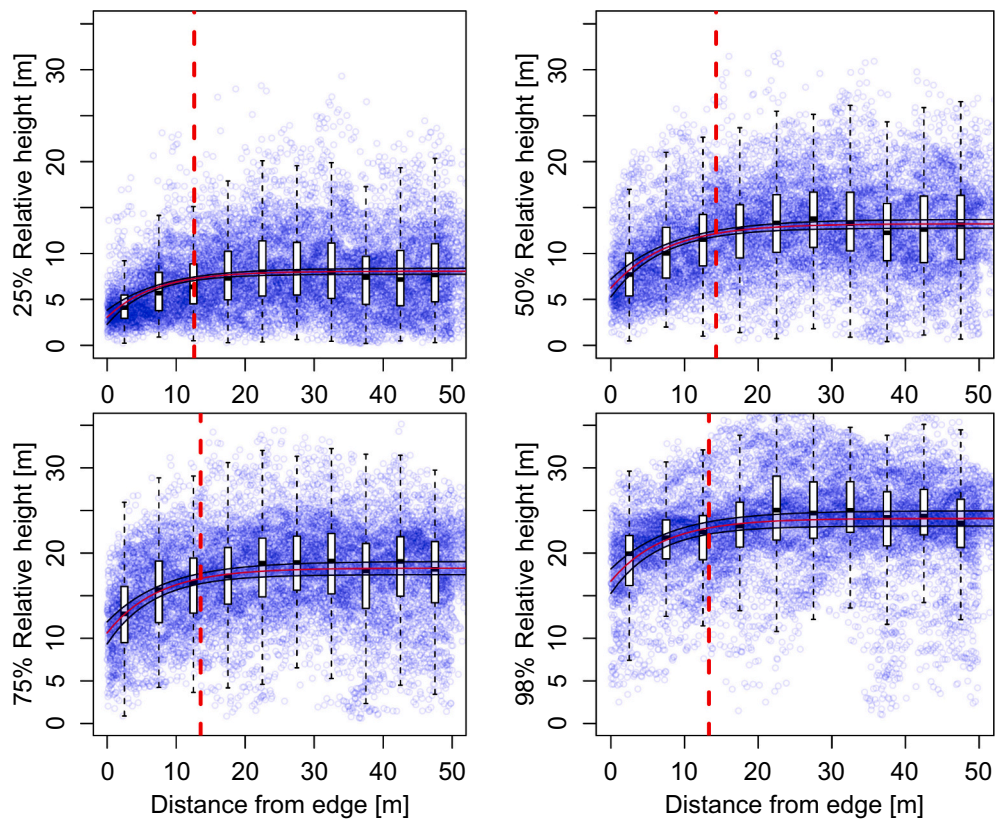


**Fig. 3.** Relative heights (RH) as percentiles of the vertical distribution of canopy points at 25, 50, 75 and 98%. Blue dots represent observed values over  $1\text{ m} \times 1\text{ m}$  columns containing the voxels. Boxplots show the distribution of observed data aggregated in five-meter slices. Solid red line shows the trait distribution based on nonlinear mixed models and black lines the 95% confidence intervals. Dashed red lines show the edge effect threshold identified using piecewise linear functions, with confidence intervals of 95%. (For interpretation of the references to colour in this figure legend, the reader is referred to the web version of this article.)

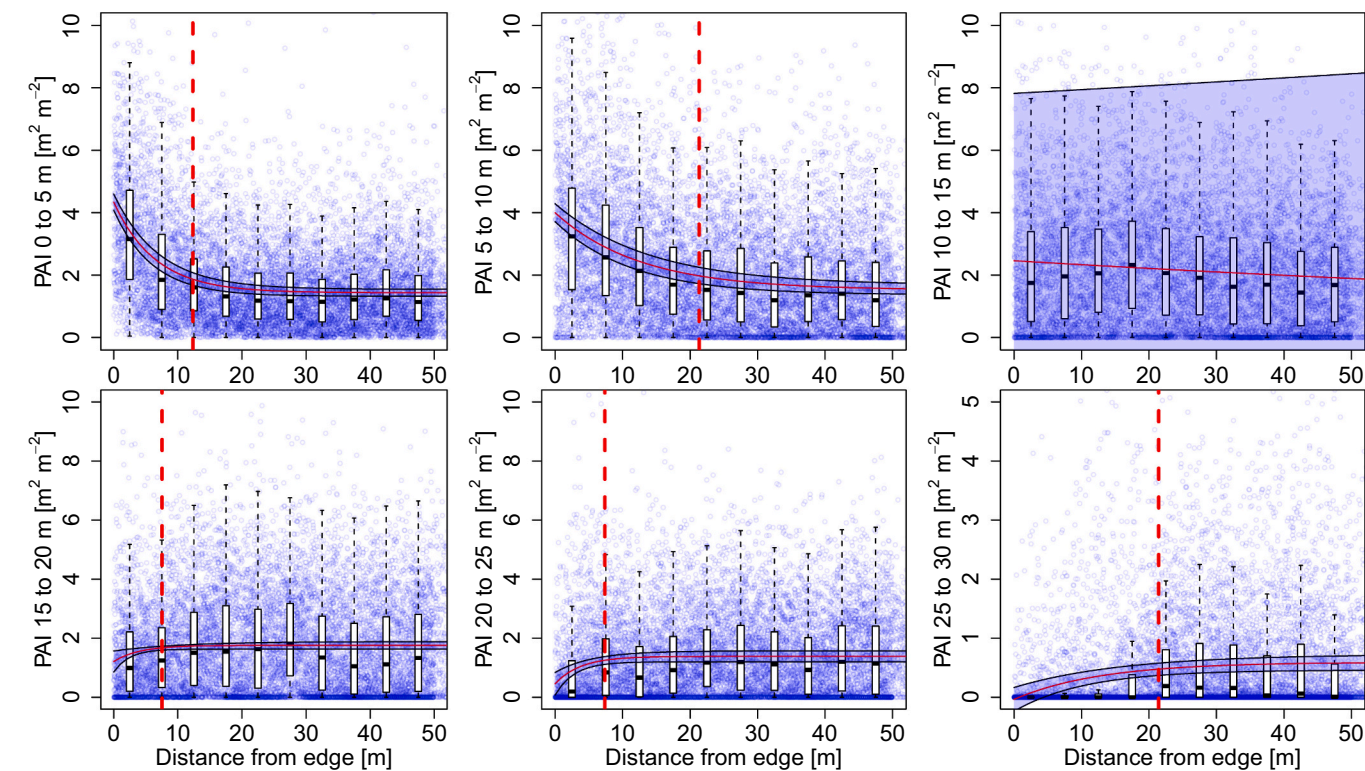


**Fig. 4.** Plant area index (PAI) per 5 m height layers from 0 to 30 m above ground. Blue dots represent observed values over  $1\text{ m} \times 1\text{ m}$  columns containing the voxels. Boxplots show the distribution of observed data aggregated in five-meter slices. Solid red and black lines show the trait distribution based on nonlinear mixed models and the 95% confidence intervals, respectively. Dashed red lines show the edge effect threshold identified using piecewise linear functions, with confidence intervals of 95%. (For interpretation of the references to colour in this figure legend, the reader is referred to the web version of this article.)

vegetation strata (between 0 and 10 m above ground) (Fig. 4). This increase can be observed up to 20 m from the edge. The understory vegetation PAI on the edges was up to 2.5-fold higher than in the centre of the transect (50 m distant from the edge). This pattern starts to change at vegetation layers between 10 and 15 m, where no significant trend in PAI is observed in the edge-interior gradient. On the top layers, above 15 m, an inverse pattern is observed, with increasing PAI from the edge to the interior of the forest. The mean PAI on the upper layers of the canopy (25 to 30 m), can be up to four times higher in the interior of the forest ( $\sim 0.45 \text{ m}^2 \text{ m}^{-2}$ ) than in the edge of the forest fragments ( $\sim 0.11 \text{ m}^2 \text{ m}^{-2}$ ).

The variation of the total PAI along the edge gradient indicate an overall increase of PAI towards the edge (Fig. 5a). The magnitude of the changes is however more subtle when compared to the ones observed in separated layers. The mean total PAI at the edge of fragments was approximately  $11 \text{ m}^2 \text{ m}^{-2}$ , compared to  $8 \text{ m}^2 \text{ m}^{-2}$  at 50 m from the edge. These results thus demonstrate that assessments that do not consider the height-stratified edge effects on forest canopies can mask more pronounced changes occurring in the edges of fragments.

FHD only changed in the very edge (0 to 3 m) of the forests (Fig. 5b), even though other structural changes were observed up to 20 m from the forest edge (Figs. 3 and 4), indicating that these changes are not related to the effective number of canopy layers. In particular, vegetation close to the forest edge was more bottom-heavy than vegetation in the interior of the forests. CR, which quantifies the relative difference in height at which the bottom 25% and the bottom 98% of the plant material is reached, clearly increased towards the forest interior, especially in the first 20 m (Fig. 5c). The mean CR in the first 5 m of the transect was approximately 20% higher than in the interior of the forest.

To evaluate how the changes in structural traits affected the structural diversity of forest edges, we evaluated the n-dimensional hypervolume formed by the traits (Fig. 6). The hypervolumes were constructed using the RH at 25, 50, and 98%, as well as PAI 0–5, PAI 5–10, PAI 20–25 and PAI 25–30 (i.e.  $n = 7$ ), which were shown to be the traits mostly affected by the edge effects. Fig. 6a shows how the structural traits hypervolume changed from the centre to the edge of the fragments. The results show a consistent shift in the similarity of hypervolumes from forest interior to edge both with the Jaccard similarity index and with the Sørensen similarity index (Fig. 6b and c). Edge effects have thus led to long-term shifts in the forest structural diversity and structural niche, up to 20 m distance from the edges.

Finally, to further understand how tree demography contributed to the changes in structural traits, we used the TLS data to carry out an exhaustive counting of all trees with DBH above 5 cm along the seven transects. We observed an increase in tree density closer to the edges

(Fig. 7a). The density of trees in the first 10 m of the edge is approximately 25% higher than in the interior of the fragment, at 50 m from the edge. This difference was mostly driven by small trees with DBH smaller than 10 cm (Fig. 7b). These results are aligned with the observed decrease in canopy height at the edge of forest fragments, indicating that the overall canopy structure is dominated by smaller and shorter trees.

#### 4. Discussion

High-density TLS data provide a fresh three-dimensional perspective on the forest fragmentation effects on Amazonian forests that can be separated across vertical strata. These data allowed a detailed characterization of the spatial distribution of plant surface area within the canopy, providing an unprecedented insight on how the allocation of plant material is affected by edge effects. Furthermore, we demonstrate how edge effects disrupt the structural diversity of fragmented forests, using a Hutchinson's n-dimensional hypervolume concept (Blonder, 2018) applied to TLS derived metrics. Our results show persistent and long-term impacts of edge effects in canopy structural traits and structural diversity in forest fragments established more than 40 years ago.

The depth of edge effects on individual structural traits varied considerably. While changes in the height distribution and layering of plant material in the vertical profile were observed only in the first 15 m from the edges, significant changes in the overall PAI could be detected up to 35 m from the edge (Fig. 5). It is important to note, however, that our results are focused on structural attributes. Other attributes, such as microclimate (Camargo and Kapos, 1995; Didham and Lawton, 1999), floristic composition (Laurance et al., 2007, 2006), and canopy dynamics (Nunes et al., 2021), were previously reported to reflect edge-effects even deeper on forest fragments, within hundreds of meters from the fragment edges.

Our findings provide an additional contribution to approaches for measuring and monitoring forest degradation caused by forest fragmentation. While many of the definitions of forest degradation focus on the loss of a single property of the forest (e.g. carbon storage) (Gao et al., 2020), more comprehensive approaches aim at assessing degradation through the frame of ecological resilience (Ghazoul et al., 2015). In such approaches, if forest functionality and resilience remain unaffected, the forest is not considered to be degraded. In other words, if a forest is able to recover from disturbance events (e.g. droughts, fires, wind, or edge effects), by this definition, it should not be considered as degraded (Ghazoul et al., 2015). Our results thus provide evidence that forests at the edge of fragments undergo persistent structural changes, adding new elements for assessing the degradation of fragmented forests through the lenses of ecological resilience.

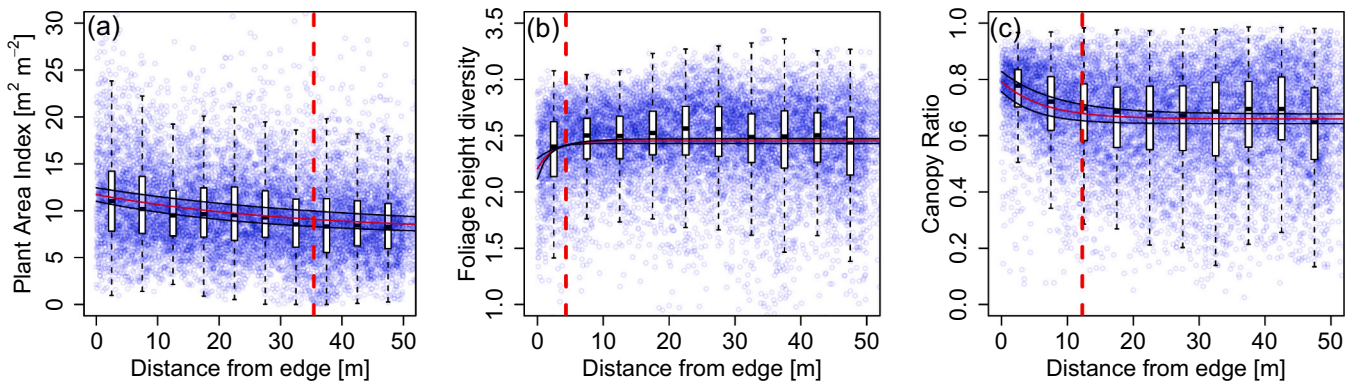


**Fig. 5.** (a) Total Plant Area Index (PAI), (b) Foliage Height Diversity (FHD) and (c) Canopy Ratio (CR) along the forest edge gradient. Blue dots represent observed values over  $1 \text{ m}^2$  columns containing the voxels. Boxplots show the distribution of observed data aggregated in five-meter slices. Solid red and black lines show the trait distribution based on nonlinear mixed models and the 95% confidence intervals, respectively. Dashed red lines show the edge effect threshold identified using piecewise linear functions, with confidence intervals of 95%. (For interpretation of the references to colour in this figure legend, the reader is referred to the web version of this article.)

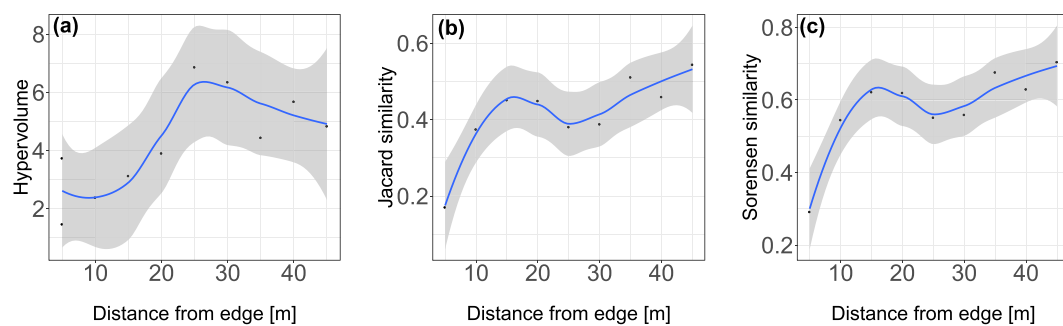


**Fig. 6.** Shifts in canopy structural diversity from edge to forest interior. (a) The hypervolume values for each five meters slice. Differences in the hypervolume between each forest slice of five meters, in comparison with the forest interior (i.e. forests with at least 50 m distance from edges), are measured using (b) the Jaccard similarity index, and (c) the Sørensen similarity index. The blue lines show conditional mean estimates using local polynomial regression fitting. The grey bands show the 95% confidence intervals. (For interpretation of the references to colour in this figure legend, the reader is referred to the web version of this article.)

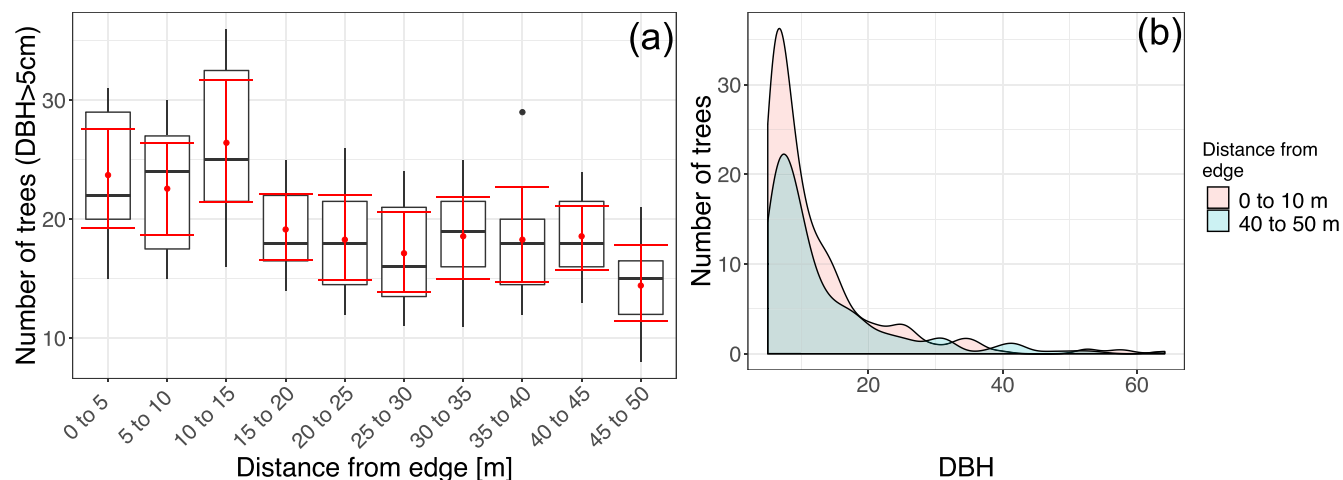


**Fig. 7.** (a) Number of trees with DBH > 5 cm identified within all seven transects, divided into slices of 5 m. The boxplots show the 25th and 75th percentiles. The red dots and lines show the mean and 95% CI, respectively. (b) Distribution of tree diameters (DBH > 5 cm) for two transect slices, one at 0 to 10 m from forest edge and the other, 40 to 50 m from the edge. (For interpretation of the references to colour in this figure legend, the reader is referred to the web version of this article.)

Currently, it is estimated that the total length of forest edges in the Amazon basin is approximately 1.5 million km (Silva Junior et al., 2020). Considering an overall edge effect depth of 20 m, we estimate that at least 30,000 km<sup>2</sup> of forests are potentially undergoing permanent changes in structural characteristics. Future deforestation and new processes of forest fragmentation in the Amazon region are likely to increase this number. It is also important to consider that the BDFFP experiment is established under controlled conditions, i.e., the matrix surrounding the fragments consists of stable secondary vegetation. More commonly, the lands surrounding forest fragments undergo intensive management, which may include, for instance, prescribed fires and cultivation of commodity crops, which can increase the penetration capacity of edge effects (Didham and Lawton, 1999). For instance, studies have shown that surface temperature increase in deforested areas converted to large-scale commodity crops can be up to three-fold higher than in small-scale farms with less intensive management (Maeda et al., 2021), increasing the potential for deeper edge-effects.

Our results also show that structural changes in forest edges have a strong vertical heterogeneity. We observed opposite PAI patterns in the lower and top layers of the forest - i.e. forest edges have higher PAD in the understory and lower PAD in the upper canopy than forest interior does. As a result, metrics that integrate structural properties over the entire vegetation column (e.g. PAI or LAI) can behave as if there were no structural effects of the disturbances along the gradient from forest edge to interior. For example, remote sensing assessments of forest disturbances are often based on LAI (or LAI proxies, such as NDVI) estimated

from satellite imagery. Such indices may not be able to capture the signal of vertically stratified horizontal heterogeneity in plant material distribution, which may lead to underestimating the extent of disturbed forests.

The lower PAD in the upper layers of forest edges is explained by a smaller number of large trees (Fig. 7). The high mortality of large trees in forest edges has been linked to a higher exposure to wind turbulence and greater desiccation stress (Laurance et al., 2006). Trees larger than 60 cm in diameter were shown to die approximately three times faster near edges than in forest interiors (Laurance et al., 2000). Changes in the light regime in gaps opened by the death of large trees, added to increased lateral light penetrating near edges, create favourable conditions to the recruitment of new individuals, mainly pioneer trees, as well as accelerated growth rates of trees and lianas that dominate the understory (Nascimento and Laurance, 2004), contribute to the higher PAI values in the edge understories.

Changes in structural traits associated with forest height (i.e. RHs) were less pronounced than those linked to PAD distribution. Changes in RH at all quantiles could only be observed up to 15 m from the edges, while changes in PAI were evident up to 35 m from the edges. Canopy height is generally easier to be measured in comparison with understory density, as it can be reliably assessed, for instance, using airborne laser scanning (Asner and Mascaro, 2014) and, more recently, spaceborne sensors (Dubayah et al., 2020). Given this fact, added to the information that a high mortality of large trees is expected in disturbed forests (Gora and Esquivel-Muelbert, 2021; Laurance et al., 2000), canopy height is

frequently used as a proxy for forest disturbances (Jucker et al., 2018). Nonetheless, our results show that, to avoid an underestimation of structural changes caused by disturbance, canopy height should not be used alone. Having said that, changes in the RH in forest edges were consistently observed in our results, and the stratification of relative heights can also provide a useful overview on changes in the spatial allocation of plants in the forest edges.

Our results were based on very high-resolution TLS data, providing the most detailed representation of structural changes in Amazonian forest edges to date. These characteristics serve at least two important purposes. First, it provides a benchmark in the characterization of structural changes in Amazonian forest edges, as the three-dimensional forest representation provided by the TLS allows a detailed characterization of both understory and upper canopy. Second, it identifies important metrics for monitoring structural characteristics of forests affected by edge effects, leading to approaches for upscaling disturbance assessments using airborne or spaceborne sensors. This is particularly timely, given the recent advent of the Global Ecosystem Dynamics Investigation (GEDI) mission (Dubayah et al., 2020).

GEDI was launched and installed on board the International Space Station in December of 2018. The mission is expected to sample about 4% of the Earth's land surface, providing an unprecedented overview on the structure and biomass of forests (Dubayah et al., 2020). Nonetheless, to take full advantage of these data, it is crucial for GEDI estimates to be benchmarked with ground data, particularly in dense tropical forests, where the characterization of understory structure by spaceborne sensors is challenging. Our approach used similar structural variables as the ones provided by GEDI level 2 and 3 products, thus providing strong evidence that GEDI data, combined with ground-based TLS data, holds large potential to be applied for assessing forest disturbances linked to edge effects. GEDI has currently collected thousands of samples throughout the Amazon basin. The sampling characteristics of GEDI (i.e. along track beams spaced by 60 m), as well as its footprint of 25 m, do not allow a transect-based design as presented in this study. However, the multiple overpasses are likely to cover a large range of representative conditions, including different distances from edges and degrees of disturbances.

Given that the retrieval of forest structural traits with TLS can be done without carrying out a floristic inventory of the forest, this approach has potential to be upscaled to other areas in Amazonian forests. In our study, the region where the data was collected, and the size of the fragments, accounted for a small fraction of the variability in our results (less than 3% on average) (Table S2 in the supplementary material). However, the importance of the biogeographical region in explaining structural trait variability is likely to increase when areas outside Central Amazonia are considered, as metrics such as canopy height and mean PAI vary strongly across the Amazon basin (Gorgens et al., 2021). Hence, expanding this approach to other geographical regions will need to account for this natural variability, requiring, for instance, a normalization of the traits. It is, however, feasible to assume that over dense evergreen forests, the overall characteristics of disturbances on canopy structure will remain similar. For instance, even though mean canopy height varies substantially across the Amazon (Sawada et al., 2015), we expect that, due to the higher mortality of larger trees, forests under the influence of edge effects will have relatively lower canopy height in comparison with adjacent forests distant from edges (Almeida et al., 2019a, 2019b; Silva Junior et al., 2020). Likewise, although the mean plant area does vary significantly throughout the Amazon, it is expected that changes in the light regime and floristic composition in forest edges lead to a consistent relative increase in the understory plant density.

## 5. Conclusions

In this study, we evaluated structural traits of fragmented Amazonian forests based on 624 terrestrial laser scanning measurements,

providing a detailed overview on the impacts of fragmentation on the three-dimensional distribution of forest plant material. We report changes in the structural diversity of forest edges formed 40 years ago, demonstrating persistent impacts of edge effects on metrics closely linked to energy harvesting and light use efficiency. Although most forest structural metrics showed edge effects, traits related to plant material allocation were more strongly affected than traits related to canopy height. The vertically integrated plant area index (PAI) showed strong edge effects, but we demonstrated that the use of this metric for assessing forest disturbance can be deceptive, given the divergent response from the forest understory (higher PAI closer to the edge) and the upper canopy (lower PAI closer to the edge). We also show that Foliage Height Diversity (FHD), which reflects the effective number of canopy layers, was lower at the very edge of the forest but soon returned to values similar to the forest interior, even though the actual vertical distribution of plant material continued to change. To allow a more solid interpretation of the changes in structural traits, we analysed the tree size distribution along the studied transects, showing a large increase in the number of trees ( $DBH \geq 5$  cm) close to the edges. This increase was driven by a larger number of small trees ( $5 \leq DBH < 10$  cm). Finally, our results provide a benchmark for assessing regional and pan-tropical disturbances caused by fragmentation, as the approach based on structural traits present large potential for being upscaled across other biogeographical regions. By clarifying the long-term impacts of edge effects on structural vegetation properties, our results contribute to a broader understanding of ecosystem resilience in forest edges, leading to a more robust interpretation of disturbances in fragmented ecosystems.

## Declaration of Competing Interest

The authors declare that they have no known competing financial interests or personal relationships that could have appeared to influence the work reported in this paper.

## Acknowledgments

This study was funded by the Academy of Finland (decision numbers 318252, 319905 and 340175). This publication is number 833 of the Technical Series of the Biological Dynamics of Forest Fragment Forest (BDFFP). Y.M.M. was supported by a research grant from the Royal Society through the Newton International Fellowship funding, grant number NF170036 and HPC-Europa3 (process n: HPC17TA3RL) supported by European Commission H2020. KC was funded by the European Union's Horizon 2020 research and innovation programme under the Marie Skłodowska-Curie grant agreement No 835398. GZ was funded by the Danish Council for Independent Research - Natural Sciences (#9040-00136B). G.V. received support from "Investissement d'Avenir" grant managed by Agence Nationale de la Recherche (CEBA, ref. ANR-10-LABX-25-01).

## Appendix A. Supplementary data

Supplementary data to this article can be found online at <https://doi.org/10.1016/j.rse.2022.112895>.

## References

- Akaike, H., 1974. A New Look at the Statistical Model Identification. In: Parzen, E., Tanabe, K., Kitagawa, G. (Eds.), Selected Papers of Hirotugu Akaike. Springer Series in Statistics (Perspectives in Statistics). Springer, New York, NY. [https://doi.org/10.1007/978-1-4612-1694-0\\_16](https://doi.org/10.1007/978-1-4612-1694-0_16).
- Almeida, D., Stark, S.C., Schiatti, J., Camargo, J.L.C., Amazonas, N.T., Gorgens, E.B., Rosa, D.M., Smith, M.N., Valbuena, R., Saleska, S., Andrade, A., Mesquita, R., Laurance, S.G., Laurance, W.F., Lovejoy, T.E., Broadbent, E.N., Shimabukuro, Y.E., Parker, G.G., Lefsky, M., Silva, C.A., Brancalion, P.H.S., 2019a. Persistent effects of fragmentation on tropical rainforest canopy structure after 20 yr of isolation. *Ecol. Appl.* 29, 1221–1235. <https://doi.org/10.1002/eap.1952>.

- Almeida, D., Stark, S.C., Shao, G., Schietti, J., Nelson, B.W., Silva, C.A., Gorgens, E.B., Valbuena, R., de Papa, D.A., Brancalion, P.H.S., 2019b. Optimizing the remote detection of tropical rainforest structure with airborne lidar: leaf area profile sensitivity to pulse density and spatial sampling. *Remote Sens. Environ.* 11, 92. <https://doi.org/10.3390/rs11010092>.
- Andersen, H.-E., Reutebuch, S.E., McGaughey, R.J., D'Oliveira, M.V.N., Keller, M., 2014. Monitoring selective logging in western Amazonia with repeat lidar flights. *Remote Sens. Environ.* 151, 157–165. <https://doi.org/10.1016/j.rse.2013.08.049>.
- Asner, G.P., Mascaro, J., 2014. Mapping tropical forest carbon: calibrating plot estimates to a simple LiDAR metric. *Remote Sens. Environ.* 140, 614–624. <https://doi.org/10.1016/j.rse.2013.09.023>.
- Barlow, J., França, F., Gardner, T.A., Hicks, C.C., Lennox, G.D., Berenguer, E., Castello, L., Economo, E.P., Ferreira, J., Guénard, B., Gontijo Leal, C., Isaac, V., Lees, A.C., Parr, C.L., Wilson, S.K., Young, P.J., Graham, N.A.J., 2018. The future of hyperdiverse tropical ecosystems. *Nature* 559, 517–526. <https://doi.org/10.1038/s41586-018-0301-1>.
- Bates, D., Mächler, M., Bolker, B., Walker, S., 2015. Fitting linear mixed-effects models using lme4. *J. Stat. Softw.* 67. <https://doi.org/10.18637/jss.v067.i01>.
- Bazezew, M.N., Hussin, Y.A., Kloosterman, E.H., 2018. Integrating airborne LiDAR and terrestrial laser scanner forest parameters for accurate above-ground biomass/carbon estimation in Ayer Hitam tropical forest, Malaysia. *Int. J. Appl. Earth Obs. Geoinf.* 73, 638–652. <https://doi.org/10.1016/j.jag.2018.07.026>.
- Béland, M., Widlowski, J.-L., Fournier, R., Côté, J.-F., Verstraete, M.M., 2011. Estimating leaf area distribution in savanna trees from terrestrial LiDAR measurements. *Agric. For. Meteorol.* 151 (9), 1252–1266.
- Blonder, B., 2018. Hypervolume concepts in niche- and trait-based ecology. *Ecography (Cope.)* 41, 1441–1455. <https://doi.org/10.1111/ecog.03187>.
- Blonder, B., 2019. *Hypervolume: High Dimensional Geometry and Set Operations Using Kernel Density Estimation, Support Vector Machines, and Convex Hulls*.
- Blonder, B., Morrow, C.B., Maitner, B., Harris, D.J., Lamanna, C., Viole, C., Enquist, B.J., Kerkhoff, A.J., 2018. New approaches for delineating n-dimensional hypervolumes. *Methods Ecol. Evol.* 9, 305–319. <https://doi.org/10.1111/2104-210X.12865>.
- Brinck, K., Fischer, R., Groeneveld, J., Lehmann, S., Dantas De Paula, M., Pütz, S., Sexton, J.O., Song, D., Huth, A., 2017. High resolution analysis of tropical forest fragmentation and its impact on the global carbon cycle. *Nat. Commun.* 8, 14855. <https://doi.org/10.1038/ncomms14855>.
- Calders, K., Adams, J., Armston, J., Bartholomeus, H., Bauwens, S., Bentley, L.P., Chave, J., Danson, F.M., Demol, M., Disney, M., Gaulton, R., Krishna Moorthy, S.M., Levick, S.R., Saarinen, N., Schaaf, C., Stovall, A., Terryn, L., Wilkes, P., Verbeeck, H., 2020. Terrestrial laser scanning in forest ecology: expanding the horizon. *Remote Sens. Environ.* 251, 112102. <https://doi.org/10.1016/j.rse.2020.112102>.
- Camargo, J.L.C., Kapos, V., 1995. Complex edge effects on soil moisture and microclimate in central Amazonian forest. *J. Trop. Ecol.* 11, 205–221. <https://doi.org/10.1017/S026646740000866X>.
- Díaz, S., Kattge, J., Cornelissen, J.H.C., Wright, I.J., Lavorel, S., Dray, S., Reu, B., Kleyer, M., Wirth, C., Colin Prentice, I., Garnier, E., Bönnisch, G., Westoby, M., Poorter, H., Reich, P.B., Moles, A.T., Dickie, J., Gillison, A.N., Zanne, A.E., Chave, J., Joseph Wright, S., Sheremet Ev, S.N., Jactel, H., Baraloto, C., Cerabolini, B., Pierce, S., Shipley, B., Kirkup, D., Casanoves, F., Joswig, J.S., Günther, A., Falczuk, V., Rüger, N., Mahecha, M.D., Gorné, L.D., 2016. The global spectrum of plant form and function. *Nature* 529, 167–171. <https://doi.org/10.1038/nature16489>.
- Didham, R.K., Lawton, J.H., 1999. Edge structure determines the magnitude of changes in microclimate and vegetation structure in tropical forest fragments. *Biotropica* 31, 17. <https://doi.org/10.2307/2663956>.
- Disney, M., 2019. Terrestrial Li <sc>DAR</sc> : a three-dimensional revolution in how we look at trees. *New Phytol.* 222, 1736–1741. <https://doi.org/10.1111/nph.15517>.
- d'Oliveira, M.V.N., Reutebuch, S.E., McGaughey, R.J., Andersen, H.-E., 2012. Estimating forest biomass and identifying low-intensity logging areas using airborne scanning lidar in Antimary State Forest, Acre State, Western Brazilian Amazon. *Remote Sens. Environ.* 124, 479–491. <https://doi.org/10.1016/j.rse.2012.05.014>.
- Drake, J.B., Knox, R.G., Dubayah, R.O., Clark, D.B., Condit, R., Blair, J.B., Hofton, M., 2003. Above-ground biomass estimation in closed canopy Neotropical forests using lidar remote sensing: factors affecting the generality of relationships. *Glob. Ecol. Biogeogr.* 12, 147–159. <https://doi.org/10.1046/j.1466-822X.2003.00010.x>.
- Dubayah, R.O., Sheldon, S.L., Clark, D.B., Hofton, M.A., Blair, J.B., Hurt, G.C., Chazdon, R.L., 2010. Estimation of tropical forest height and biomass dynamics using lidar remote sensing at La Selva, Costa Rica. *J. Geophys. Res. Biogeosciences* 115. <https://doi.org/10.1029/2009JG000933> n/a-n/a.
- Dubayah, R., Blair, J.B., Goetz, S., Fatoyinbo, L., Hansen, M., Healey, S., Hofton, M., Hurt, G., Kellner, J., Luthcke, S., Armston, J., Tang, H., Duncanson, L., Hancock, S., Jantz, P., Marselis, S., Patterson, P.L., Qi, W., Silva, C., 2020. The global ecosystem dynamics investigation: high-resolution laser ranging of the earth's forests and topography. *Sci. Remote Sens.* 1, 100002. <https://doi.org/10.1016/j.srs.2020.100002>.
- Duong, V.H., Lindenbergh, R., Pfeifer, N., Vosselman, G., 2008. Single and two epoch analysis of ICESat full waveform data over forested areas. *Int. J. Remote Sens.* 29, 1453–1473. <https://doi.org/10.1080/01431160701736372>.
- Ehlers Smith, Y.C., Ehlers Smith, D.A., Ramesh, T., Downs, C.T., 2017. The importance of microhabitat structure in maintaining forest mammal diversity in a mixed land-use mosaic. *Biodivers. Conserv.* 26, 2361–2382. <https://doi.org/10.1007/s10531-017-1360-6>.
- Enquist, B.J., West, G.B., Brown, J.H., 2009. Extensions and evaluations of a general quantitative theory of forest structure and dynamics. *Proc. Natl. Acad. Sci.* 106, 7046–7051. <https://doi.org/10.1073/pnas.0812303106>.
- Fahay, R.T., Atkins, J.W., Gough, C.M., Hardiman, B.S., Nave, L.E., Tallant, J.M., Nadehoffer, K.J., Vogel, C., Scheuermann, C.M., Stuart-Haenpts, E., Haber, L.T., Fotis, A.T., Ricart, R., Curtis, P.S., 2019. Defining a spectrum of integrative trait-based vegetation canopy structural types. *Ecol. Lett.* 22, 2049–2059. <https://doi.org/10.1111/ele.13388>.
- Froidevaux, J.S.P., Zellweger, F., Bollmann, K., Jones, G., M.K., 2016. ObristFrom field surveys to LiDAR: shining a light on how bats respond to forest structure. *Remote Sens. Environ.* 175, 242–250.
- Gao, Y., Skutsch, M., Panque-Gálvez, J., Ghilardi, A., 2020. Remote sensing of forest degradation: a review. *Environ. Res. Lett.* 15, 103001. <https://doi.org/10.1088/1748-9326/abaad7>.
- Ghazoul, J., Burivalova, Z., Garcia-Ulloa, J., King, L.A., 2015. Conceptualizing Forest degradation. *Trends Ecol. Evol.* 30, 622–632. <https://doi.org/10.1016/j.tree.2015.08.001>.
- Gora, E.M., Esquivel-Muelbert, A., 2021. Implications of size-dependent tree mortality for tropical forest carbon dynamics. *Nat. Plants* 7, 384–391. <https://doi.org/10.1038/s41477-021-00879-0>.
- Gorgens, E.B., Nunes, M.H., Jackson, T., Coomes, D., Keller, M., Reis, C.R., Valbuena, R., Rosette, J., Almeida, D.R.A., Gimenez, B., Cantinho, R., Motta, A.Z., Assis, M., Souza Pereira, F.R., Spanner, G., Higuchi, N., Ometto, J.P., 2021. Resource availability and disturbance shape maximum tree height across the Amazon. *Glob. Chang. Biol.* 27, 177–189. <https://doi.org/10.1111/gcb.15423>.
- Grantham, H.S., Duncan, A., Evans, T.D., Jones, K., Beyer, H., Shuster, R., Walston, J., Ray, J., Robinson, J., Callow, M., Clements, T., Costa, H., DeGenninis, A., Elsen, P., Ervin, J., Franco, P., Goldman, E., Goetz, S., Hansen, A., Hofsvang, E., Jantz, P., Jupiter, S., Kang, A., Langhammer, P., Laurance, W.F., Lieberman, S., Linkie, M., Malhi, Y., Maxwell, S., Mendez, M., Mittermeier, R., Murray, N., Possingham, H., Radachowsky, J., Samper, C., Silverman, J., Shapiro, A., Strassburg, B., Stevens, T., Stokes, E., Taylor, R., Tear, T., Tizard, R., Venter, O., Visconti, P., Wang, S., Watson, J.E.M., 2020. Only 40% of the World's Forests are in Good Health. *bioRxiv* 2020.03.05.978858. <https://doi.org/10.1101/2020.03.05.978858>.
- Grau, E., Durrieu, S., Fournier, R., Gastellu-Etchegorry, J.-P., Yin, T., 2017. Estimation of 3D vegetation density with terrestrial laser scanning data using voxels. A sensitivity analysis of influencing parameters. *Remote Sens. Environ.* 191, 373–388. <https://doi.org/10.1016/j.rse.2017.01.032>.
- Hansen, M.C., Wang, L., Song, X.-P., Tyukavina, A., Turubanova, S., Potapov, P.V., Stehman, S.V., 2020. The fate of tropical forest fragments. *Sci. Adv.* 6. <https://doi.org/10.1126/sciadv.aax8574> eaax8574.
- Heiskanen, J., Korhonen, L., Hietanen, J., Pellikka, P.K.E., 2015. Use of airborne lidar for estimating canopy gap fraction and leaf area index of tropical montane forests. *Int. J. Remote Sens.* 36, 2569–2583. <https://doi.org/10.1080/01431161.2015.1041177>.
- Jucker, T., Bouriaud, O., Coomes, D.A., 2015. Crown plasticity enables trees to optimize canopy packing in mixed-species forests. *Funct. Ecol.* 29, 1078–1086. <https://doi.org/10.1111/1365-2435.12428>.
- Jucker, T., Asner, G.P., Dalponte, M., Brodrick, P.G., Philipson, C.D., Vaughn, N.R., Teh, Y.A., Breelford, C., Burleson, D.F.R.P., Deere, N.J., Ewers, R.M., Kvashnica, J., Lewis, S.L., Malhi, Y., Milne, S., Nilus, R., Pfeifer, M., Phillips, O.L., Qie, L., Renneboog, N., Reynolds, G., Riutta, T., Struebig, M.J., Svátek, M., Turner, E.C., Coomes, D.A., 2018. Estimating aboveground carbon density and its uncertainty in Borneo's structurally complex tropical forests using airborne laser scanning. *Biogeosciences* 15, 3811–3830. <https://doi.org/10.5194/bg-15-3811-2018>.
- LaRue, E.A., Hardiman, B.S., Elliott, J.M., Fei, S., 2019. Structural diversity as a predictor of ecosystem function. *Environ. Res. Lett.* 14, 114011. <https://doi.org/10.1088/1748-9326/ab49bb>.
- Laurance, W.F., Delamónica, P., Laurance, S.G., Vasconcelos, H.L., Lovejoy, T.E., 2000. Rainforest fragmentation kills big trees. *Nature* 404, 836. <https://doi.org/10.1038/35009032>.
- Laurance, W.F., Lovejoy, T.E., Vasconcelos, H.L., Bruna, E.M., Didham, R.K., Stouffer, P.C., Gascon, C., Bierregaard, R.O., Laurance, S.G., Sampaio, E., 2002. Ecosystem decay of Amazonian Forest fragments: a 22-year investigation. *Conserv. Biol.* 16, 605–618. <https://doi.org/10.1046/j.1523-1739.2002.01025.x>.
- Laurance, W.F., Nascimento, H.E.M., Laurance, S.G., Andrade, A., Ribeiro, J.E.L.S., Giraldo, J.P., Lovejoy, T.E., Condit, R., Chave, J., Harms, K.E., D'Angelo, S., 2006. Rapid decay of tree-community composition in Amazonian forest fragments. *Proc. Natl. Acad. Sci.* 103, 19010–19014. <https://doi.org/10.1073/pnas.0609048103>.
- Laurance, W.F., Nascimento, H.E.M., Laurance, S.G., Andrade, A., Ewers, R.M., Harms, K.E., Luizão, R.C.C., Ribeiro, J.E., 2007. Habitat fragmentation, variable edge effects, and the landscape-divergence hypothesis. *PLoS One* 2, e1017. <https://doi.org/10.1371/journal.pone.0001017>.
- Laurance, W.F., Camargo, J.L.C., Luizão, R.C.C., Laurance, S.G., Pimm, S.L., Bruna, E.M., Stouffer, P.C., Bruce Williamson, G., Benítez-Malvido, J., Vasconcelos, H.L., Van Houtan, K.S., Zartman, C.E., Boyle, S.A., Didham, R.K., Andrade, A., Lovejoy, T.E., 2011. The fate of Amazonian forest fragments: a 32-year investigation. *Biol. Conserv.* 144, 56–67. <https://doi.org/10.1016/j.bioc.2010.09.021>.
- Laurance, W.F., Camargo, J.L.C., Fearnside, P.M., Lovejoy, T.E., Williamson, G.B., Mesquita, R.C.G., Meyer, C.F.J., Bobrowiec, P.E.D., Laurance, S.G.W., 2018. An Amazonian rainforest and its fragments as a laboratory of global change. *Biol. Rev.* 93, 223–247. <https://doi.org/10.1111/brv.12343>.
- Lesak, A.A., Radloff, V.C., Hawbaker, T.J., Pidgeon, A.M., Gobakken, T., Contrucci, K., 2011. Modeling forest songbird species richness using LiDAR-derived measures of forest structure. *Remote Sens. Environ.* 115, 2823–2835. <https://doi.org/10.1016/j.rse.2011.01.025>.
- Ma, L., Zheng, G., Ying, Q., Hancock, S., Ju, W., Yu, D., 2021. Characterizing the three-dimensional spatiotemporal variation of forest photosynthetically active radiation using terrestrial laser scanning data. *Agric. For. Meteorol.* 301–302, 108346. <https://doi.org/10.1016/j.agrformet.2021.108346>.

- MacArthur, R.H., MacArthur, J.W., 1961. On bird species diversity. *Ecology* 42, 594–598. <https://doi.org/10.2307/1932254>.
- Maeda, E.E., Abera, T.A., Siljander, M., Aragão, L.E.O.C., de Moura, Y.M., Heiskanen, J., 2021. Large-scale commodity agriculture exacerbates the climatic impacts of Amazonian deforestation. *Proc. Natl. Acad. Sci.* 118, e2023787118 <https://doi.org/10.1073/pnas.2023787118>.
- Mammola, S., 2019. Assessing similarity of n-dimensional hypervolumes: which metric to use? *J. Biogeogr.* 46, 2012–2023. <https://doi.org/10.1111/jbi.13618>.
- Meeussen, C., Govaert, S., Vanmeete, T., Calders, K., Bollmann, K., Brunet, J., Cousins, S.A.O., Diekman, M., Graae, B.J., Hedwall, P.-O., Krishna Moorthy, S.M., Iacopetti, G., Lenoir, J., Lindmo, S., Orczevski, A., Ponette, Q., Plue, J., Selvi, F., Spicher, F., Tolosano, M., Verbeeck, H., Verheyen, K., Vangansbeke, P., De Frenne, P., 2020. Structural variation of forest edges across Europe. *For. Ecol. Manag.* 462, 117929 <https://doi.org/10.1016/j.foreco.2020.117929>.
- Nascimento, H.E.M., Laurance, W.F., 2004. Biomass dynamics in Amazonian Forest fragments. *Ecol. Appl.* 14, 127–138. <https://doi.org/10.1890/01-6003>.
- Nilson, T., 1971. A theoretical analysis of the frequency of gaps in plant stands. *Agric. Meteorol.* 8, 25–38.
- Nunes, M.H., Jucker, T., Riutta, T., Svátek, M., Kvásnica, J., Rejžek, M., Matula, R., Majalap, N., Ewers, R.M., Swinfield, T., Valbuena, R., Vaughn, N.R., Asner, G.P., Coomes, D.A., 2021. Recovery of logged forest fragments in a human-modified tropical landscape during the 2015–16 El Niño. *Nat. Commun.* 12, 1526. <https://doi.org/10.1038/s41467-020-20811-y>.
- Ordway, E.M., Asner, G.P., 2020. Carbon declines along tropical forest edges correspond to heterogeneous effects on canopy structure and function. *Proc. Natl. Acad. Sci.* 117, 7863–7870. <https://doi.org/10.1073/pnas.1914420117>.
- Parrish, J.D., Braun, D.P., Unnasch, R.S., 2003. Are we conserving what we say we are? Measuring ecological integrity within protected areas. *Bioscience* 53, 851–860. [https://doi.org/10.1641/0006-3568\(2003\)053\[0851:AWCWWS\]2.0.CO;2](https://doi.org/10.1641/0006-3568(2003)053[0851:AWCWWS]2.0.CO;2).
- Pimont, F., Allard, D., Soma, M., Dupuy, J.-L., 2018. Estimators and confidence intervals for plant area density at voxel scale with T-LiDAR. *Remote Sens. Environ.* 215, 343–370. <https://doi.org/10.1016/j.rse.2018.06.024>.
- Reich, P.B., 2012. Key canopy traits drive forest productivity. *Proc. R. Soc. B Biol. Sci.* 279, 2128–2134. <https://doi.org/10.1098/rspb.2011.2270>.
- Ross, J., 1981. *The Radiation Regime and Architecture of Plant Stands*. Springer Netherlands, Dordrecht.
- Sawada, Y., Suwa, R., Jindo, K., Endo, T., Oki, K., Sawada, H., Arai, E., Shimabukuro, Y.E., Celes, C.H.S., Campos, M.A.A., Higuchi, F.G., Lima, A.J.N., Higuchi, N., Kajimoto, T., Ishizuka, M., 2015. A new 500-m resolution map of canopy height for Amazon forest using spaceborne LiDAR and cloud-free MODIS imagery. *Int. J. Appl. Earth Obs. Geoinf.* 43, 92–101. <https://doi.org/10.1016/j.jag.2015.04.003>.
- Schneider, F.D., Morsdorf, F., Schmid, B., Petchey, O.L., Hueni, A., Schimel, D.S., Schaepman, M.E., 2017. Mapping functional diversity from remotely sensed morphological and physiological forest traits. *Nat. Commun.* 8, 1441. <https://doi.org/10.1038/s41467-017-01530-3>.
- Schneider, F.D., Ferraz, A., Hancock, S., Duncanson, L.I., Dubayah, R.O., Pavlick, R.P., Schimel, D.S., 2020. Towards mapping the diversity of canopy structure from space with GEDI. *Environ. Res. Lett.* 15, 115006 <https://doi.org/10.1088/1748-9326/ab9e99>.
- Silva Junior, C.H.L., Aragão, L.E.O.C., Anderson, L.O., Fonseca, M.G., Shimabukuro, Y.E., Vancutsem, C., Achard, F., Beuchle, R., Numata, I., Silva, C.A., Maeda, E.E., Longo, M., Saatchi, S.S., 2020. Persistent collapse of biomass in Amazonian forest edges following deforestation leads to unaccounted carbon losses. *Sci. Adv.* 6 <https://doi.org/10.1126/sciadv.aaz8360> eaaz8360.
- Silva Pedro, M., Rammer, W., Seidl, R., 2017. Disentangling the effects of compositional and structural diversity on forest productivity. *J. Veg. Sci.* 28, 649–658. <https://doi.org/10.1111/jvs.12505>.
- Sonderegger, D., 2020. SiZer: Significant Zero Crossings.
- Stark, S.C., Enquist, B.J., Saleska, S.R., Leitold, V., Schietti, J., Longo, M., Alves, L.F., Camargo, P.B., Oliveira, R.C., 2015. Linking canopy leaf area and light environments with tree size distributions to explain Amazon forest demography. *Ecol. Lett.* 18, 636–645. <https://doi.org/10.1111/ele.12440>.
- Tabarelli, M., Cardoso da Silva, J.M., Gascon, C., 2004. Forest fragmentation, synergisms and the impoverishment of neotropical forests. *Biodivers. Conserv.* 13, 1419–1425. <https://doi.org/10.1023/B:BIOC.0000019398.36045.1b>.
- Tuomisto, H., 2017. Defining, Measuring, and Partitioning Species Diversity \*, in: Reference Module in Life Sciences. Elsevier. <https://doi.org/10.1016/B978-0-12-809633-8.02377-3>.
- Valbuena, R., Packalén, P., Martí'n-Fernández, S., Maltamo, M., 2012. Diversity and equitability ordering profiles applied to study forest structure. *For. Ecol. Manag.* 276, 185–195. <https://doi.org/10.1016/j.foreco.2012.03.036>.
- Verbeeck, H., Bauters, M., Jackson, T., Shenkin, A., Disney, M., Calders, K., 2019. Time for a plant structural economics spectrum. *Front. For. Glob. Chang.* 2 <https://doi.org/10.3389/ffgc.2019.00043>.
- Vincent, G., Antin, C., Laurans, M., Heurtebize, J., Durrieu, S., Lavallee, C., Dauzat, J., 2017. Mapping plant area index of tropical evergreen forest by airborne laser scanning. A cross-validation study using LAI2200 optical sensor. *Remote Sens. Environ.* 198, 254–266. <https://doi.org/10.1016/j.rse.2017.05.034>.
- Vincent, G., Pimont, F., Verley, P., 2021. A Note on PAD/LAD Estimators Implemented in AMAPVox 1.7. <https://doi.org/10.23708/1AJNMP>.
- Wilkes, P., Lau, A., Disney, M., Calders, K., Burt, A., Gonzalez de Tanago, J., Bartholomeus, H., Brede, B., Herold, M., 2017. Data acquisition considerations for terrestrial laser scanning of forest plots. *Remote Sens. Environ.* 196, 140–153. <https://doi.org/10.1016/j.rse.2017.04.030>.